Dyes and Pigments 113 (2015) 227–238

Contents lists available at ScienceDirect

Dyes and Pigments

journal homepage: www.elsevier.com/locate/dyepig

Tuning optical and electronic properties of poly(4,4'-triphenylamine vinylene)s by post-modification reactions

Mircea Grigoras*, Ana Maria Catargiu, Teofilia Ivan, Loredana Vacareanu, Boris Minaev, Evgeniy Stromylo

[a] "P. Poni" Institute of Macromolecular Chemistry, Electroactive Polymers Department, 41A Gr. Ghica Voda Alley, Iasi 700487, Romania
[b] Bogdan Khmelnitsky National University, Organic Chemistry Department, bv. Shevchenko 81, Cherkasy 18031, Ukraine

ARTICLE INFO

Article history:
Received 25 May 2014
Received in revised form
18 August 2014
Accepted 18 August 2014
Available online 27 August 2014

Keywords:
Polyarylenevinylenes
Synthesis
Phenylethynyl and pyridylethynyl substituents
Chemical modification
Tune optical and electrochemical properties
Density functional theory calculations

ABSTRACT

New triphenylamine-based polyarylenevinylenes with pendant phenylethynyl- and 3-pyridylethynyl substituents were synthesized by Stille polycondensation of *trans*-1,2-bis(tributylstannyl)ethene with two new ethynyl substituted triphenylamine monomers, i.e., *N,N*-bis(4-iodophenyl)-4'-(phenylethynyl) phenylamine and *N,N*-bis(4-iodophenyl)-4'-(3-pyridylethynyl) phenylamine. The polymers were characterized by spectral methods and cyclic voltammetry and their properties were compared with those of the unsubstituted poly(4,4'-triphenylamine vinylene). Chemical post-modifications of the polymers by tetracyanoethylene addition to the triple bond, and quaternization of pyridyl group with accent on the fine-tuning of the optical and electrochemical properties were also studied. Density functional theory calculations provide a reliable interpretation of the observed spectra and electrochemical data.

1. Introduction

Poly(arylene vinylene)s (PPVs) represent a well studied class of materials among conjugated polymers due to their interesting scientific aspects of synthesis and very useful properties for many optoelectronic applications [1]. The seminal work of the Cambridge group in 1990 [2] evidenced the presence of light emitting properties in PPVs and has renewed scientific interest for this class of polymers [3–5]. Now, the potential application of PPVs in the next generation of full-color flat panel displays is recognized and many researchers are interested to obtain new polymer structures with high emission efficiency. Other interesting applications are in the organic field effect transistors [6,7] and photovoltaic cells [8,9]. The main routes used to tune the electro-physical properties of PPVs are based on the use of new monomer structures or new catalytic systems or synthesis methods. A simple and effective approach for tuning the optoelectronic properties of conjugated polymers is through modification of functional pendant groups with acceptor compounds, but this method is less studied until now. Nurulla et al. have modified polyarylenes containing alternating fluorene and 4-phenylethynyl substituted triphenylamine groups by Diels–Alder reaction of the triple bond with tetraphenylcyclopentadienone [10] or by oxidation followed by addition of *o*-phenylenediamine to obtain quinoxaline pendant units [11]. The pendant aldehyde groups can be modified with nitrile compounds, 1,3-diethyl-2-thiobarbituric acid or 3-dicyanovinylindan-1-one to introduce side chain acceptor groups [12–14]. Depending on the acceptor moieties of the side chain, the absorption spectra and energy gap can be fine-tuned. Li et al. has modified conjugated polymers containing carbazole and triphenylamine in the main chain by reaction of pendant aldehyde groups with malononitrile and ethyl cyanoacetate [15]. We have also synthesized triphenylamine-based polyarylenes with pendant –CHO and CH_2OH functions and modified their optical properties by Knoevenagel reaction with cyanoacetic acid or phenyl isocyanate addition [16,17]. In all cases either a bathochromic shift of the absorption and emission peaks was observed or new bands due to the charge-transfer complexes formed between donor and acceptor groups. These compounds show intramolecular charge-transfer (ICT) interactions and efficient electron transfer from donor to acceptor upon photoexcitation, being promising candidates for building of the dye-sensitized and bulk heterojunction (BHJ) solar cells.

* Corresponding author.
E-mail address: grim@icmpp.ro (M. Grigoras).

http://dx.doi.org/10.1016/j.dyepig.2014.08.016
0143-7208/

Furthermore, we intend to extend this method to poly-arylenevinylenes containing triphenylamine substituted in the free *para* position with phenylethynyl- and 3-pyridylethynyl groups. The electron-rich triple bond could be post-modified by: (a) addition of tetracyanoethylene [18–26], (b) cycloaddition of tetraphenylcyclopentadienone [10], (c) transformation into a quinoxaline acceptor group [11], while pyridyl group can be (d) protonated or quaternized with alkyl bromides [27], with final effects on the main chain conjugation length. Routes (a) and (d) will be explored to tune the optical and electronic properties of PPVs. So, in this paper we report the synthesis and spectroscopic and electrochemical characterization of poly [4,4'-(4″-phenylethynyl)-triphenylamine vinylene] and poly[4,4'-(4″-3-pyridylethynyl)-triphenylamine vinylene] obtained by Stille polycondensation. A comparative analysis of the optical and electronic properties of parent and chemical modified polymers will be presented and correlated using time-dependent density functional theory (TD-DFT) calculations. The TD-DFT analysis can provide a link between structure and NMR, absorption and luminescence spectra of such polymers [28,29].

2. Experimental

2.1. Materials

Triphenylamine, 3-ethynylpyridine, triethylamine, $Pd(PPh_3)_4$, PPh_3, CuI, *trans*-1,2-*bis*(tributylstannyl)ethene, all from Aldrich and phenylacetylene (Fluka), were used as received. Other reactants and solvents are obtained from commercial sources and used as received or dried by known methods. Tetrabutylammonium perclorate ($(C_4H_9)_4NClO_4$) was used as supporting electrolyte in electrochemical studies. All manipulations were carried out under an inert atmosphere using the Schlenk technique.

2.2. Measurements

FT-IR spectra were recorded in KBr pellets on a DIGILAB-FTS 2000 spectrometer. ^1H NMR and ^{13}C NMR spectra were recorded at room temperature on a Bruker Avance DRX-400 spectrometer operating respectively at 400 MHz (for ^1H) and 100.39 MHz (for ^{13}C) as solutions in $CDCl_3$ or DMSO-d_6 and chemical shifts are reported in ppm and referenced to TMS as internal standard or DMSO-d_5. UV–Vis and fluorescence measurements were carried out in $CHCl_3$ solution (spectrophotometric grade) or as a film on quartz glass, on a Specord 200 spectrophotometer and Perkin Elmer LS 55 apparatus, respectively. The fluorescence quantum yields were determined by the integrating sphere method using an FLS 980 spectrometer and $CHCl_3$ as solvent upon excitation with $\lambda_{ex} = 400$ nm. Differential scanning calorimetry (DSC) and thermogravimetric analyses (TGA) were carried our in a TGA/DTA STA 449 F1 Netzsch (Germany) at a heating rate of 10 °C/min in a nitrogen flow. The relative molecular weights were determined by gel permeation chromatography (GPC) using a PL-EMD 950 Evaporative Mass Detector instrument and polystyrene standards for the calibration plot and chloroform (1 mL/min) as solvent.

The cyclic voltammograms (CV) were recorded using a Bioanalytical System, Potentiostat–Galvanostat (BAS 100B/W). The electrochemical cell was equipped with three electrodes: a working electrode (disk shape Pt electrode, $\Phi = 1.6$ mm), an auxiliary electrode (platinum wire), and a reference electrode (consisted of a silver wire coated with AgCl). Before experiments, Pt electrode was polished between each set of experiments with aluminium oxide powder on a polishing cloth, and then was sonicated in a mixture of detergent and methanol for 5 min and then rinsed with a large amount of doubly distilled water. The reference electrode (Ag/Ag^+) was calibrated at the beginning of the experiments by running the CV of ferrocene as the internal standard in an identical cell without any compound in the system ($E_{1/2} = 0.40$ V versus the Ag/AgCl). Prior to the each experiment, the Bu_4NClO_4 solutions were deoxygenated by passing dry nitrogen gas for 10 min. All measurements were performed at room temperature (25 °C) under nitrogen atmosphere.

2.3. Monomers and polymers synthesis

The synthetic routes for triphenylamine-based monomers starting from triphenylamine, are outlined in Scheme 1. 4,4',4″-Trisiodotriphenylamine and 4,4'-diiodotriphenylamine (**1**) were obtained by iodination of triphenylamine with KI/KIO_3 in acetic acid, using known methods [30,31]. The Sonogashira coupling of 4,4',4″-trisiodotriphenylamine with phenylacetylene and 3-pyridylacetylene in the presence of catalyst [$(PPh_3)_2PdCl_2$, CuI, PPh_3] using triethylamine as solvent gave monomers **2** and **3**.

2.3.1. Synthesis of bis(4-iodophenyl)-phenylamine (*1*)

In a 250 mL two-neck round bottom flask equipped with magnetic stirrer, condenser and nitrogen inlet–outlet were introduced triphenylamine (8 g, 3.2 mmol), KI (7.19 g, 4.3 mmol), and glacial acetic acid (120 mL). The mixture was stirred in nitrogen atmosphere at 85 °C for 5 h and KIO_3 (4.60 g, 2.15 mmol) was introduced over 5 h. The mixture was precipitated in water and a dirty white compound was obtained and purified by column chromatography using ethyl acetate/hexane (1:5) as eluent. Yield: 66%, Mp = 69–70 °C. ^1H NMR ($CDCl_3$, ppm): 7.50 (4H, d, $J = 8.8$ Hz), 7.24 (2H, d, $J = 8.0$ Hz), 7.06–7.04 (3H, d + t), 6.82–6.80 (4H, d, $J = 8.8$ Hz).

2.3.2. Synthesis of N,N-bis(4-iodophenyl)-4'-(phenylethynyl) phenylamine (*2*)

In a 100 mL three-neck round bottom flask equipped with magnetic stirrer, condenser and nitrogen inlet–outlet were introduced phenylacetylene (0.47 mL, 4.3 mmol), $PdCl_2 \cdot 2PPh_3$ (0.011 g), CuI (0.018 g), PPh_3 (0.0165 g), TEA (8 mL) and reaction mixture was stirred at room temperature for 2 h. 4,4',4″-Trisiodotriphenylamine (2.678 g, 4.3 mmol) dissolved in TEA (5 mL) was added to the flask and the reaction mixture was maintained 24 h at 50–60 °C. The product was separated by precipitation in water, washed with aqueous solution 0.1 M HCl and dried. Pure yellow crystalline compound was obtained by flash chromatography using hexane as eluent. Yield = 88.4%. Mp = 74–75 °C. ESI-MS = 598.2 ($M + H^+$). IR (KBr, cm^{-1}): 3043, 2210, 1634, 1574, 1505, 1313, 1265, 1177, 1058, 1002, 912, 816,753, 689. ^1H NMR ($CDCl_3$, ppm): 7.58–7.48 (6H, m), 7.4 (2H, t), 7.35–7.30 (3H, m), 7.05–6.95 (2H, m), 6.9–6.75 (4H, m). ^{13}C NMR (CDCl3, 100.39 MHz, ppm): 146.89, 135.98, 132.84, 132.6, 131.55, 128.39, 128.17, 126.13, 123.40, 123.11, 117.55, 116.37, 89.24, 89.22.

2.3.3. Synthesis of N,N-bis(4-iodophenyl)-4'-(3-pyridylethynyl) phenylamine (*3*)

In a 50 mL three-neck round bottom flask equipped with magnetic stirrer, condenser and nitrogen inlet–outlet were introduced 3-ethynylpyridine (0.165 g, 1.6 mmol), $PdCl_2 \cdot 2PPh_3$ (0.056 g, 0.08 mmol), CuI (0.03 g, 0.16 mmol), PPh_3 (0.04 g, 0.16 mmol), triethylamine (15 mL) and tetrahydrofuran (5 mL). The mixture was stirred in nitrogen atmosphere at 50–60 °C for an hour after that 4,4',4″-trisiodotriphenylamine (1 g, 1.6 mmol) dissolved in a mixture of TEA (5 mL) and THF (5 mL) was added. Then the mixture was stirred at 80 °C when the solution color turned out in time from yellow to red and some solids are deposited on the flask's walls. After 24 h the mixture was precipitated in water, filtrated and dried. The pure orange compound **3** was obtained by silicagel

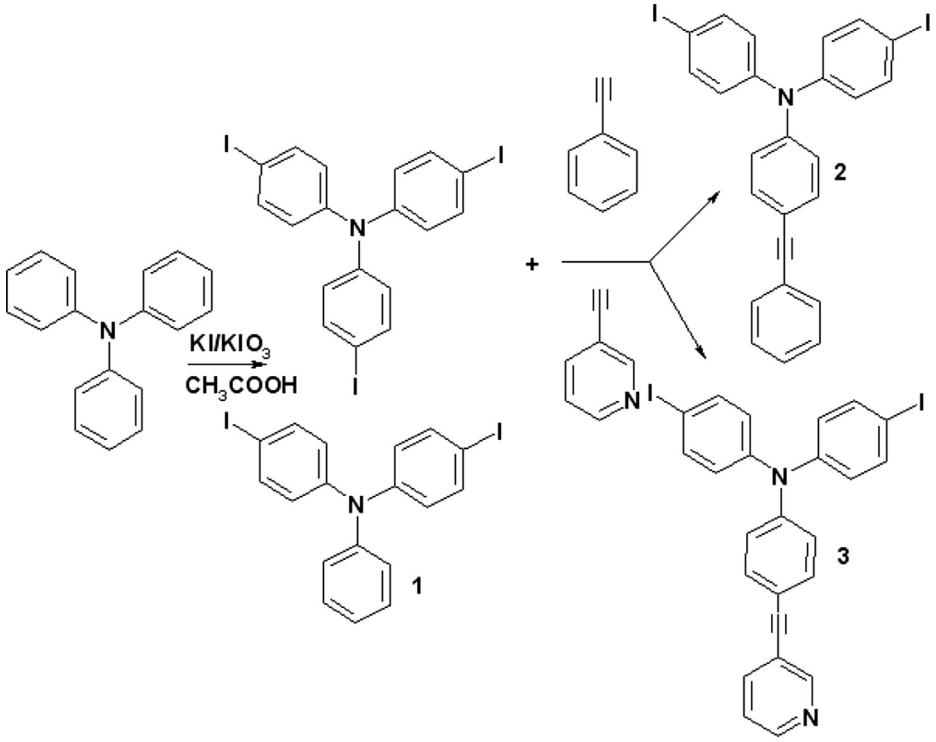

Scheme 1. Synthesis of *p*-ethynyl substituted diiodotriphenylamine derivatives.

chromatography using ethyl acetate/hexane (1:4 vol/vol) as eluent. Yield: 46.6%. Mp = 80 °C. ESI-MS = 599.2 ($M + H^+$). IR (KBr, cm^{-1}): 3032, 2212, 1647, 1599, 1575, 1504, 1479, 1404, 1314, 1284, 1265, 1179, 1142, 1001, 818, 803, 700. ^1H NMR ($CDCl_3$, ppm): 8.75 (1H, pyridyl), 8.54 (1H, d, H, pyridyl), 7.81 (1H, d, pyridyl, $J = 8.0$ Hz), 7.57 (4H, d, $J = 8.8$ Hz), 7.41 (2H, d, $J = 8.4$ Hz), 7.28 (1H, t, pyridyl), 7.01 (2H, d, $J = 8.4$ Hz), 6.85 (4H, d, $J = 8.8$ Hz).

2.3.4. Synthesis of polymers

The synthesis of homopolymer **P1** was previously described [17]. Yield: 64.9%. FTIR (KBr, cm^{-1}): 3025, 2923, 1594, 1507, 1489, 1314, 1280, 1178, 1106, 958, 828, 730, 695; ^1H NMR ($CDCl_3$, ppm): 6.8–7.6 (aromatic and vinylene protons); ^{13}C NMR ($CDCl_3$, 100.39 MHz, δ, ppm): 147.32, 146.77, 132.21, 129.42, 129.32, 129.12, 127.21, 126.71, 125.36, 124.65, 123.99, 123.23.

A typical procedure is described for synthesis of polymer **P2** (Scheme 2).

P2: In a 50 mL two-necked-flask were added monomer **2** (0.48 g, 0.8 mmol), *trans*-1,2-bis(tributylstannyl)ethene (0.47 mL, 0.8 mmol), and dry toluene (10 mL). After degassed by argon bubbling for 15 min, the solution of $Pd(PPh_3)_4$ (9.3 mg, 0.008 mmol) in dry toluene (2 mL) was added. The reaction mixture was degassed again for 30 min. Then the reaction mixture was heated and stirred to 90 °C for 24 h. The mixture was precipitated in methanol, filtrated and dried. The polymer was completely dissolved in chloroform and reprecipitated in methanol. Yield = 70.0%. FTIR (KBr, cm^{-1}): 3028, 2954, 2922, 2849, 2212, 1595, 1505, 1317, 1285, 1178, 1103, 1009, 960, 826, 754, 692; ^1H NMR ($CDCl_3$, ppm): 6.80–7.60; ^{13}C NMR ($CDCl_3$, 100.39 MHz, δ, ppm): 152.13, 148.31, 146.70, 146.06, 138.42, 138.24, 132.81, 127.46, 127.07, 126.51, 124.95, 123.01, 117.43, 92,72 and 86.30 (CC triple bond).

P3: Yield = 58.1%. FTIR (KBr, cm^{-1}): 3030, 2958, 2923, 2849, 2214, 1598, 1505, 1317, 1285, 1179, 1098, 1020, 961, 804, 703; ^1H NMR ($CDCl_3$, ppm): 5.20, 5.67, 6.80–7.80, 8.53, 8.75; ^{13}C NMR

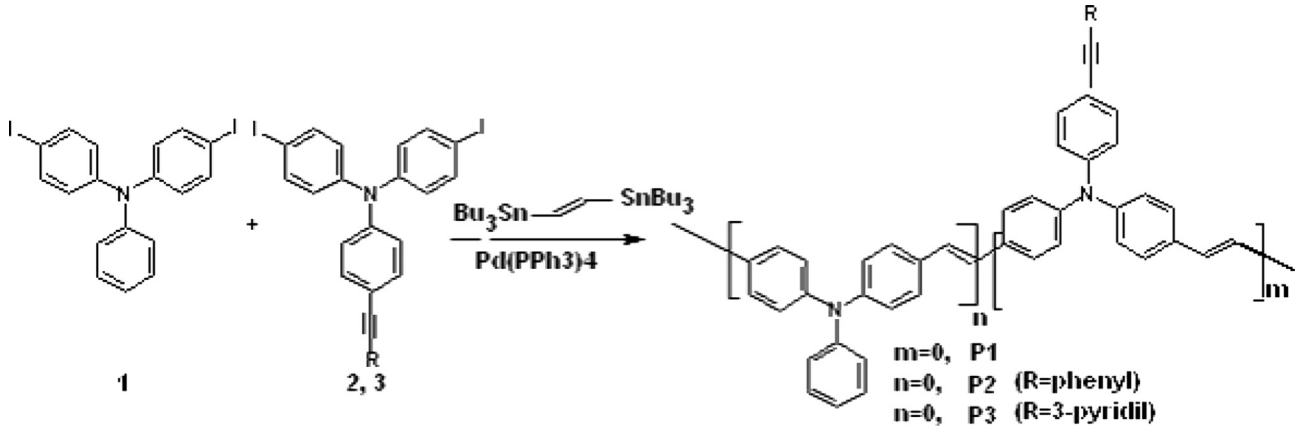

Scheme 2. Synthesis of TPA-based PAVs by Stille coupling polymerization.

Table 1
Polymerization results, optical and thermal properties of polymers.

Sample	Yield (%)	M_n (PDI)	λ_{abs} (nm)		E_g^{opt} solution (eV)	λ_{em} (nm)	Φ_F (%)	Td_5 (°C)	Char yield at 700 °C (%)
			Solution	Film					
P1	64.9	4140 (1.99)	313, 357, 409	308, 410	2.52	460	37.9	363	76.3
P2	70.0	4870 (2.20)	277, 403	374, 418 (sh)	2.53	459	31.6	300	79.4
P2m	74.2	5670 (2.12)	326, 400, 514	332, 407, 525	2.34	461	7.2		
P3	58.1	4580 (2.50)	303, 405	373	2.52	451	<1	290	75.2
P3m	79.7	5020 (2.35)	310, 408	315, 410	2.51	453	<1		

($CDCl_3$, 100.39 MHz, δ, ppm): 152.13, 148.31, 147.48, 146.70, 146.61, 145.10, 138.24, 132.81, 127.46, 127.07, 126.90, 126.50, 124.95, 123.01, 120.76, 116.21, 92.90 and 86.64 (triple bond CC).

2.3.5. Chemical modification of polymers

P2m: **P2** (25 mg) dissolved in CH_2Cl_2 (20 mL) was treated with tetracyanoethylene (9 mg), and stirred at room temperature in nitrogen atmosphere for 20 h. The initial yellow-greenish color of solution turned out dark-red. After concentration, the solution was precipitated in hexane. Yield: 74.2%. FTIR (KBr, cm^{-1}): 3034, 2959, 2923, 2222, 1593, 1504, 1325, 1285, 1182, 1010, 964, 825, 756, 696; ^1H NMR ($CDCl_3$, ppm): 7.8–6.7 (triphenylamine, phenyl and vinylene protons).

P3m: To a solution of **P3** (0.1 g) in $CHCl_3$, (6 mL), CH_3I (1 mL) was added and the red solution was gentle refluxed in nitrogen atmosphere for 3 h, cooled and precipitated in methanol to obtain a dark-red polymer (Yield; 0.11 g, 79.7%). FTIR (KBr, cm^{-1}): 3431, 3021, 2921, 2853, 2201, 1594, 1503, 1315, 1265, 1174, 1003, 960, 816, 744, 666; ^1H NMR (DMSO-d_6, ppm): 9.35, 9.02, 8.71, 8.22, 7.67–6.96, 4.40 (–CH_3), 3.4 and 2.5 (from solvent).

3. Results and discussion

3.1. Synthesis and characterization

Monomers used in synthesis of the functional PPVs are obtained starting from triphenylamine, according to the reactions outlined in Scheme 1.

Iodination of triphenylamine was carried out with KI/KIO_3 in acetic acid and depending on the molar ratios between reactants, 4,4'-diiodo- or 4,4',4″-triiodo-TPA were obtained [30,31]. The Sonogashira coupling of equimolar mixtures of tris(4-iodophenyl) amine with phenylacetylene or 3-pyridylacetylene in presence of Pd/Cu catalysts led to monomers **2** and **3**. The structures of the monomers **2** and **3** were proved by FT-IR, ^1H NMR and MS (see Section 2). DSC studies have evidenced only melting processes on the first heating scan while the pendant triple bonds of **2** and **3** are stable until 150 °C that means they does not participate in the Stille polycondensation reaction carried out at 90 °C. On the cooling scan no crystallization was observed, both monomers remained in an amorphous state. These compounds were used as monomers in Stille coupling reaction [32,33] with *trans*-1,2-bis(tributylstannyl) ethene to obtain homopolymers **P2** and **P3** (Scheme 2). A poly(-arylene vinylene) containing only triphenylamine groups and vinylene units (**P1**) was used as a control sample and its synthesis was previously reported [17].

The polymers synthesized by the Stille reaction are readily soluble in common organic solvents such as chloroform, dichloromethane, THF, DMF and toluene. Polymers were obtained in good yields (58.1–79.7%) and reasonable molecular weights. The molecular weights of the polymers were determined by gel permeation chromatography (GPC). Polymers **P2** and **P3** have number-average molecular weights of 4870 g/mol and 4580 g/mol, respectively, corresponding to degrees of polymerization of about 13–15. The polydispersity index is 2.2 and 2.5, respectively. The polymer modification has led to a slight increase in molecular weights (Table 1). All polymers are colored powders, **P1** and **P2** are yellow solids, while **P3** is a bright-red solid. Compared with parent polymers, the modified polymers are more soluble in polar solvents and are dark-red colored powders.

The modification of polymers was carried out with tetracyanoethylene (TCNE) (for **P2**) or methyl iodide for **P3** (Scheme 3). The electron-rich acetylene function can be easily modified by the [2+2] cycloaddition of the strong acceptor TCNE followed by cyclo-reversion of the adduct under mild conditions leading to a new 1,1,4,4-tetracyano 1,3-butadiene derivative [34,35]. Tetracyanoethylene can also react readily by electrophilic substitution with aliphatic and aromatic amines to give tricyanovinyl compounds [36,37]. The reaction was carried in DMF at 70 °C and an excess of TCNE. However, in our case, the presence of side product containing 1,2,2-tricyanovinyl group resulted by electrophilic substitution of TPA is less probable because the TCNE was not used in excess and the reactive *para* position of TPA is blocked by substitution with phenylethynyl group.

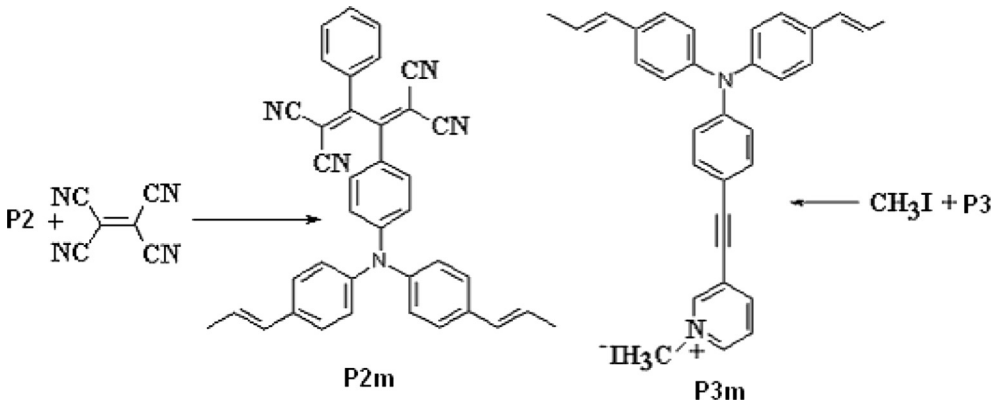

Scheme 3. Chemical modification of functional PPVs by post-reactions.

Infrared spectra of all polymers are shown in Fig. 1. All spectra show an absorption in the range 955–965 cm^{-1}, which is assigned to the out of plane C–H bending vibration of the *trans* vinyl linkage. For polymers **P2** and **P3** the presence of weak bands around 2212 cm^{-1} and 2214 cm^{-1}, respectively, assigned to the triple bond stretching vibration supports the formation of polymers with pendant triple bonds. This absorption band disappears in the spectrum of polymer **P2m**, being replaced by a new peak at 2222 cm^{-1} (assigned to CN stretching vibration) indicating the presence of nitrile linkage and confirms the addition of tetracyanoethylene to the triple bond.

^{1}H NMR spectra of the pristine and modified polymers are shown in Fig. 2. As it is shown in the figure the signals of the aromatic and *trans* vinylene protons appears together as a broad signal between 6.5 and 8.0 ppm. Aromatic protons in the *ortho*-position to pyridine nitrogen are downfield shifted and appear as distinct signals at 8.75 and 8.51 ppm. Weak signals at 5.17, 5.67 and 6.6 ppm can be assigned to the vinyl end group. For instance, 4-vinyl triphenylamine shows aromatic protons as a multiplet between 6.8 and 7.2 ppm while vinyl protons are positioned as two doublets at 5.08 ppm and 5.56 ppm and a quartet at 6.60 ppm.

The pendant triple bond is also clear evidenced by ^{13}C NMR spectroscopy by presence of signals between 85 and 92 ppm (see Section 2).

The addition of TCNE to triple bond does not modify significantly the form of the NMR spectrum of **P2**. However, adjacent phenyl protons are shifted at lower magnetic field (at 7.97–7.67 ppm) as a result of the strong electron-withdrawing effect from the tetracyanobutadiene group. As shown in Fig. 2, after quaternization with methyl iodide, **P3m** is more soluble in protic solvents (DMSO, DMF, THF) and in NMR spectrum (in DMSO-d_5) all pyridine protons are shifted downfield and appear at 9.32 ppm, 8.94 ppm, 8.66 ppm and 8.15 ppm due to the increasing of electron-withdrawing properties of quaternized pyridine ring.

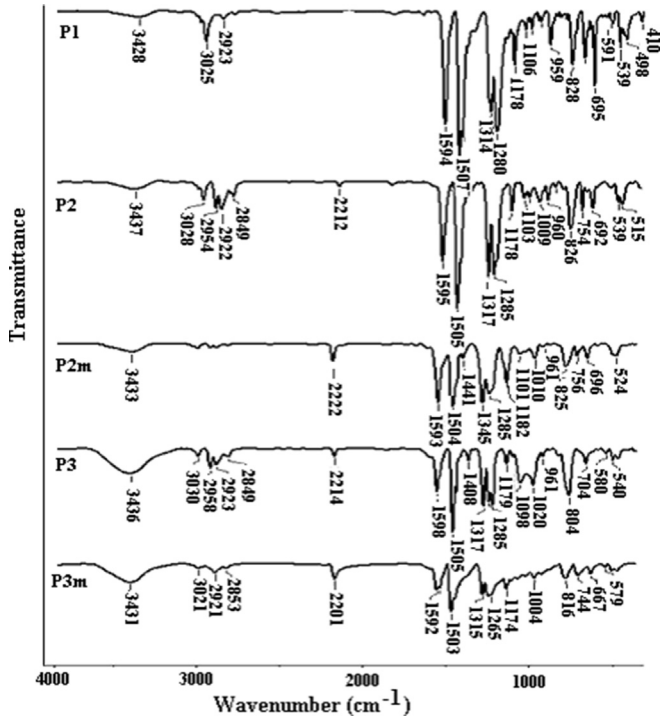

Fig. 1. FT-IR spectra (KBr pellet) of polymers: **P1**, **P2**, **P2m**, **P3** and **P3m.**

3.2. Thermal properties

Thermal properties were investigated by thermogravimetric analyses in the temperature range of 25–700 °C (TGA) and by differential scanning calorimetry (DSC) under nitrogen atmosphere. As shown in Fig. 3 polymers exhibit good thermal stability, the degradation onsets are at least up to 260 °C. The 5% weight loss temperatures were determined to be 363 (**P1**), 300 (**P2**), and 290 °C (**P3**), respectively. The char yields at 700 °C were 76.3% (**P1**), 79.4% (**P2**) and 75.2% (**P3**). DSC studies have evidenced a glass transition temperature (T_g) of 182 °C for **P1** while for others polymers no T_g were observed between 25 and 200 °C.

3.3. Optical properties

The photophysical behavior of the polymers has been studied in dilute chloroform solution (1×10^{-5} M) or in solid state as thin films obtained by drop-casting method from $CHCl_3$ or DMSO (**P3m**). The optical characteristics are summarized in Table 1. All absorption spectra show structured absorption bands, each comprising two absorption maxima in the range of 300–450 nm (Fig. 4).

The introduction of the electron-withdrawing cyano groups by addition of TCNE to the triple bond produces an intramolecular charge-transfer (ICT) interaction between triphenylamine unit and the acceptor pendant group and **P2m** shows the absorption band due to ICT complex at 514 nm in solution and 525 nm in solid state. This conclusion is completely supported by quantum chemical calculations, presented in the next chapter. The modification of **P3** by cycloaddition of TCNE to triple bond is not complete, and polymer shows IR absorptions both due to triple C≡C and C≡N bonds. The pyridyl group due to its electron-withdrawing character, decreases the reactivity of triple bond versus TCNE. **P3** modified with TCNE shows absorption in visible region with maximum shifted at 594 nm due to intramolecular charge-transfer transition. The reactivity largely depends on the electron-donating groups substituted by the alkyne moiety, and triphenylamine strong donor was found to afford the desired donor–acceptor structures in a quantitative yield at room temperature.

The fluorescence quantum yields (Φ_F) were measured for polymers **P1**–**P3** using the absolute method in which the ratio of the number of absorbed photons of a sample and the number of consequently emitted photons is directly measured. The all high-diluted $CHCl_3$ solutions were excited at 400 nm. It was noticed that the values of fluorescence quantum yields of the sample decrease from **P1** (37.9%) to **P2** (31.6%) and **P3** (7.2%). The fluorescence quantum yield for modified polymers, **P2m** and **P3m** (excited at 400 nm or $\lambda_{ICT} = 514$ nm) is very low (~1%) due to the efficient electron transfer from donor to acceptor upon photoexcitation.

The quaternized polymer **P3m** shows absorption peaks at 310 and 403 nm. The absorption band assigned to the electronic π–π* transition from the aromatic rings is red shifted by about 3 nm vs the polymer parent due to the increase of accepting properties of pyridine by quaternization. Thin films of the polymers show similar absorption spectra as compared with that in $CHCl_3$ solution, with slight red-shifted maxima while the absorption edges are shifted to longer wavelengths relative to solution spectra (Fig. 4B). The absorption edges of these polymers are 494 nm (**P1**), 500 nm (**P2**), 534 nm (**P2m**), 490 nm (**P3**) and 537 nm (**P3m**), respectively. The optical band gaps (E_g) of polymers were estimated from the absorption edge of films using the relation $E_g = 1240/\lambda_{onset}$ and used to calculate energy of LUMO level.

The PL spectra of all the polymers were also recorded in chloroform solution. The emission maxima are summarized in Table 1. The maxima of emission in solution are centered at 450–460 nm. The blue shifting of polymers **P2** and **P3** with respect to **P1**

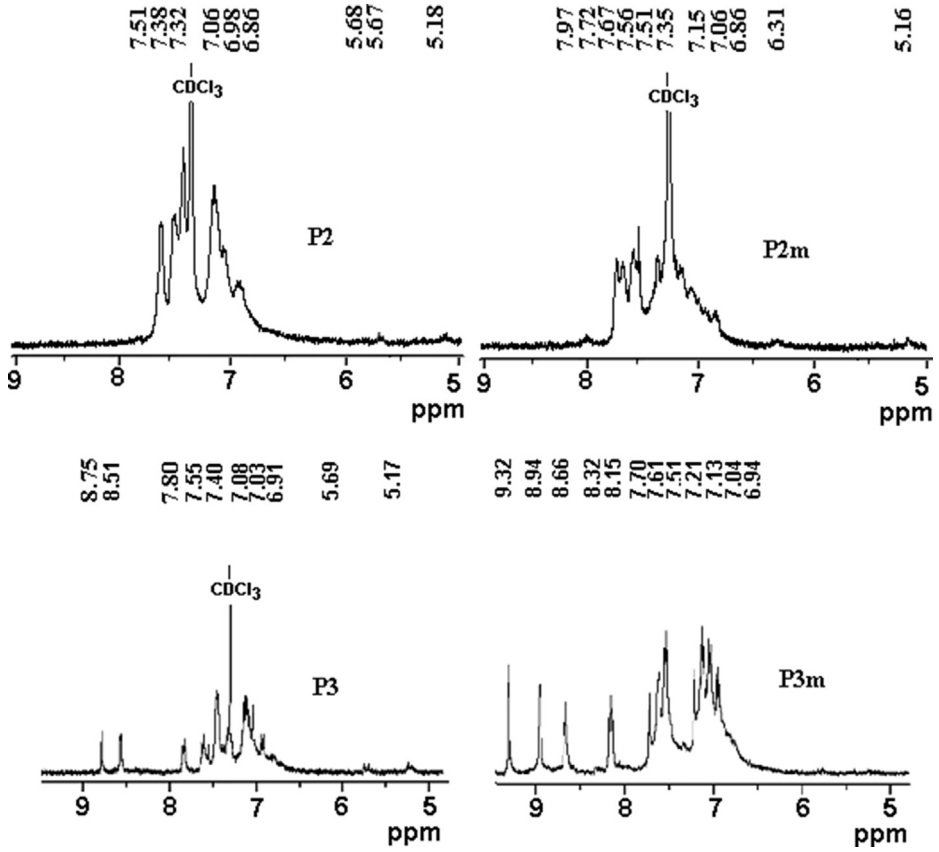

Fig. 2. ^{1}H NMR spectra ($CDCl_3$) of polymers **P2**, **P3**, **P2m** and **P3m.**

observed in UV–Vis absorptions spectra can also be also seen in the PL spectra.

Protonation of **P3** by addition of HCl to the pyridyl group results in a decrease of absorption maximum and a red shift at 408 nm when the molar ratio [HCl]/pyridine reaches 1:1.5 due to enhancing the electron-withdrawing capability of pyridinium moiety (Fig. 5).

3.4. Theoretical analysis

3.4.1. Computation details

The ground singlet-state geometry optimization of **P1**, **P2m** and **P3m** monomers, dimers and trimers was performed by the DFT/B3LYP methods [38,39] using the 6–31G(d) basis set with the GAUSSIAN 09 package [40]. The convergence criteria for geometry optimization were 2×10^{-5} Hartree for energy and 4×10^{-3} Hartree/Bohr for the force field. All the calculated vibration frequencies are found to be real, which indicates the finding of a true total energy minimum on the potential energy hypersurface. The triplet excited-state geometry was also optimized for all oligomers in order to estimate the form and size of the exciton state (assuming that singlet and triplet first excited states are similar in the orbital nature). The calculated infrared frequencies were corrected by scaling factor (0.96) for comparison with the observed IR spectra. The electronic absorption spectra and triplet excited-state energies of the studied compounds were calculated by the time-dependent (TD) DFT method using the BMK [41] functional and the same basis sets. The polarized continuum model (PCM) incorporating chloroform as a model solvent for our compounds was used in TD-DFT calculations. The same chloroform was also used as the solvent for the experimental measurements of the UV–vis spectra.

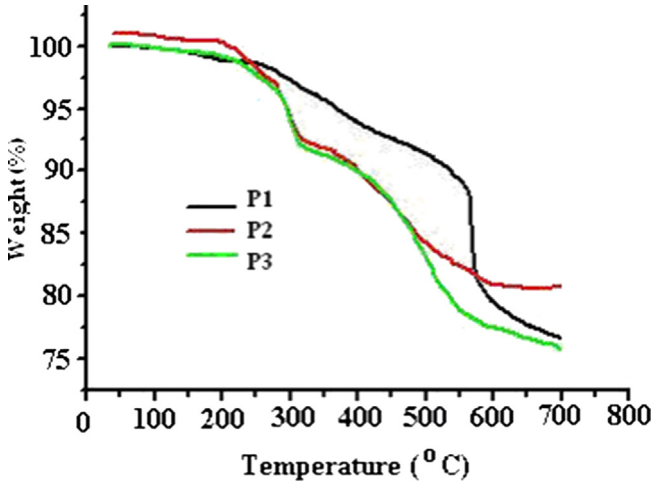

Fig. 3. TGA curves of polymers.

3.4.2. Results

The calculated infrared frequencies and intensities are in a reasonable agreement with the observed IR spectra (Fig. 1). The triple C≡C bond stretching vibrations are obtained as very weak bands around 2212 cm^{-1} and 2214 cm^{-1} for all the studied oligomers of **P2** and **P3,** respectively. Even for dimers these bands include a fine structure, which is not resolved in the observed spectra (Fig. 1). (The calculated splitting is only 0.13 cm^{-1} in the **P2** dimer.) In contrast to observation these bands are predicted to be more intense. A more complicated group of the close-lying IR transitions produces a new peak in the **P2m** compounds near 2229–2255 cm^{-1} which are assigned to C≡N stretching vibrations

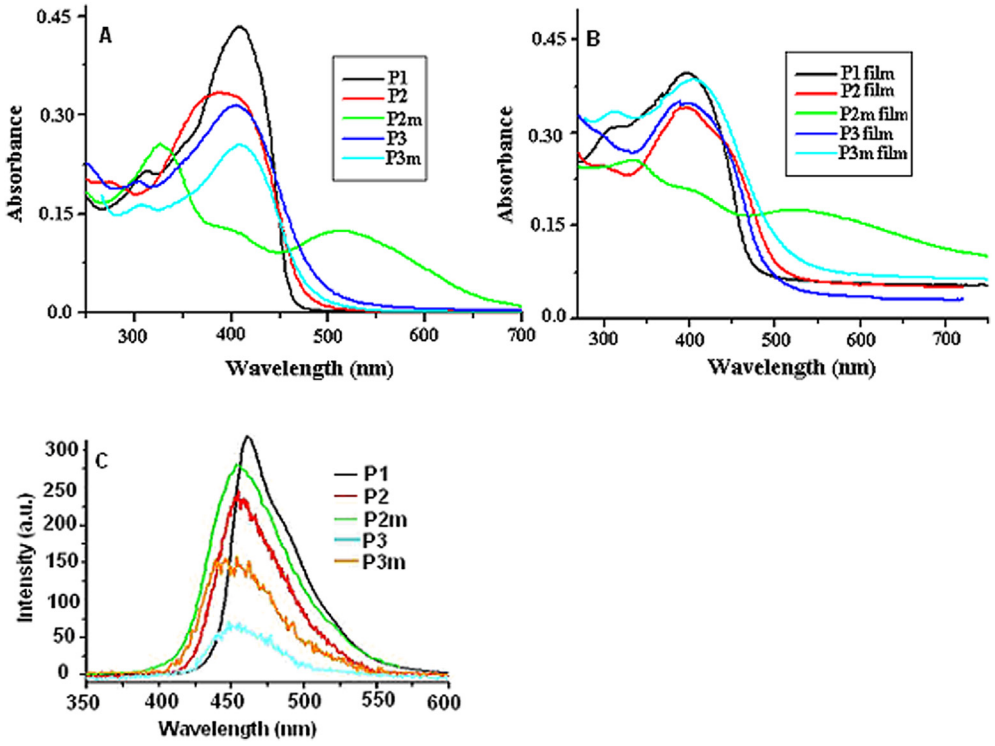

Fig. 4. Absorption spectra in solution ($CHCl_3$) (A) and solid state (B) and emission spectra (C) in solution ($CHCl_3$) of polymers **P1**, **P2**, **P2m**, **P3** and **P3m**.

of symmetric and asymmetric types. This fine structure is slightly resolved in the IR spectrum (Fig. 1) and explains the higher IR absorption intensity of the tetracyanobutadiene groups. All four calculated C≡N modes are split in such a way that they produce three close-lying bands (separated by 13 cm^{-1}) and the central one is the most intense. The central band consists of two lines of different intensity split by only 2.4 cm^{-1}. All these fine features are clearly seen in the IR spectrum of **P2m** (Fig. 1).

3.4.3. TD-DFT interpretation of the UV–visible absorption spectra

All absorption maxima in the range of 300–450 nm for compounds **P1**, **P2**, **P2m**, **P3** and **P3m** (Fig. 4) are assigned to π–π* electronic transitions in conjugated phenyl rings, most of which are non-planar to each other. As follows from geometry optimization the rings in the triphenylamine unit are oriented by a dihedral angle of 39°, nevertheless the photoactive molecular orbitals (MO) are mainly delocalized in all oligomers (Fig. 6).

Based on the triphenylamine spectrum as a reference (Fig. 6a, Table 2), absorption maxima located at around 300 nm are assigned to π–π* electronic transition from the triphenylamine unit, while the peaks located in the range 390–410 nm can be assigned to the π–π* transition of the conjugated backbone (Fig. 6b, c). The absorption maxima for **P1** appear at 409 nm and 313 nm (with a shoulder at 357 nm). All these features are well reproduced in the trimer model (Fig. 6c, Table 2). A very intense peak at 410 nm and the shoulder are in a good agreement with the experimental spectrum for the **P1** polymer (Fig. 4, Table 1). The observed UV band at 313 nm indicates lower intensity in agreement with calculation (330 nm, $f = 0.26$) as well as the far UV absorption (227 nm, Table 2).

It is interesting to see evolution of excited states in the series of oligomers of the P1 compound (Fig. 6, Table 2). With the increase of the oligomer chain the first absorption band is shifted to the visible region. This shift is very strong on going from monomer to dimer (65 nm) and diminished drastically upon further transition to the trimer (17 nm). For the tetramer we anticipate a negligibly small additional shift. According to the calculated MO levels (Fig. 6c) the orbital nature of the first band (HOMO–LUMO excitation) is the same. This transition partly includes electron density transfer from the pendant phenyl ring (which is not presented in LUMO) to the backbone. From Fig. 6c one can see that the HOMO–LUMO exciton is mostly localized on the trimer moiety. This conclusion is also supported by our PM3 calculations of the longer oligomers (Figs. S6–S8).

The growth of the polymer chain does not change the main features of the HOMO and LUMO. Thus the nature of the first absorption band is the same (but the wavelength is shifted).

TD-DFT calculations show that in **P2m** the nature of the first absorption band (536 nm, Table 2) is completely changed. This is

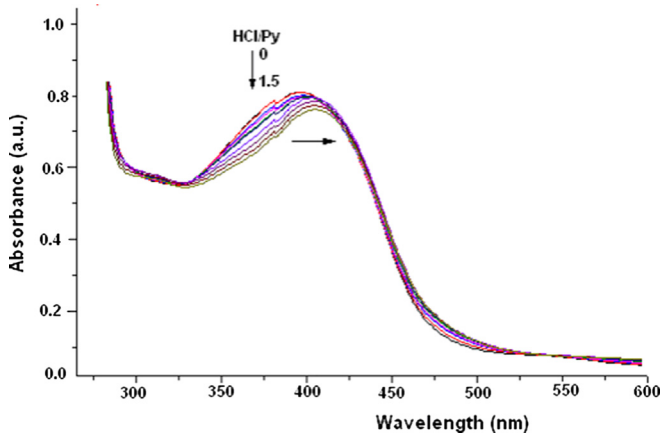

Fig. 5. Modification of UV spectrum of **P3** by protonation with HCl.

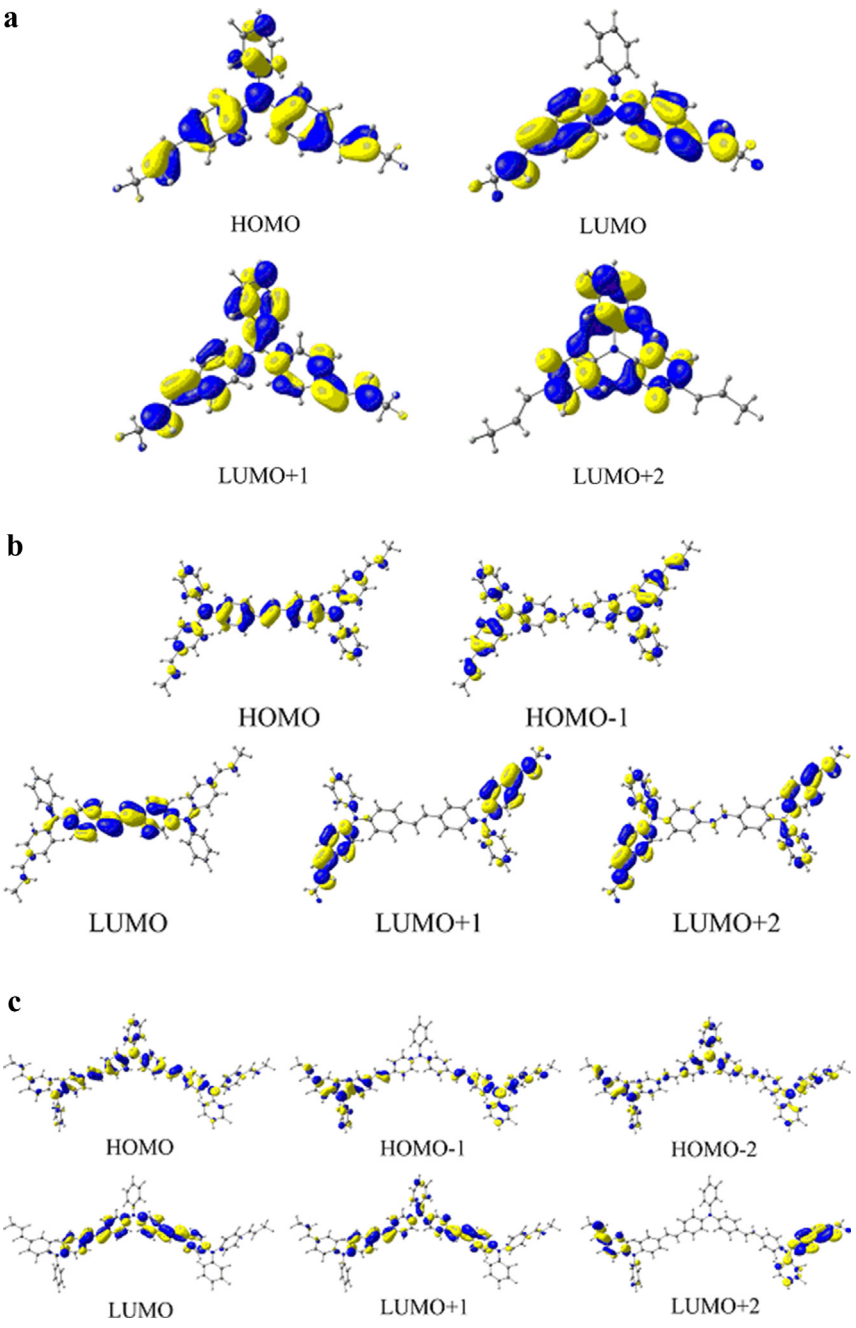

Fig. 6. (a) **P1** monomer molecule and its MOs. (b) DFT calculated MOs of **P1** dimer. (c) DFT calculated MOs of **P1** trimer.

the charge-transfer transition from the backbone to the tetracyanobutadiene groups (Fig. 7). The presence of the tetracyanobutadiene groups induces a new spectrum which is determined just by this monomer feature. It will not depend much on the polymer backbone, but mostly on the monomer characteristics. We have calculated dimer and trimer models of **P2m** by the PM3 method and this conclusion is supported to be correct.

Our TD-DFT results for the **P2m** monomer are in a good agreement with the observed absorption spectrum in the film (Tables 1 and 2). Intensity of all absorption bands is much lower than in other polymers. The second and third bands in **P2m** also demonstrate charge-transfer nature (Fig. 7) and the total spectrum is very different from the spectra of other species (Fig. 4).

We used two models for geometry optimization of the **P3m** monomer; one in the form of the pyridyl-containing cation (Fig. 8a) and the other – in the form of the salt (with the iodine atom coordination at the nitrogen site). The former model provides quite reasonable agreement with the experimental spectra upon the chain prolongation, but the salt structure failed completely. Since we have no any agreement for **P3m** with experiment for the UV–visible spectrum we conclude that the salt model is wrong. Three highest occupied molecular orbitals represent the lone pairs at the iodine anion and three charge-transfer transitions are predicted in the far visible region (the difference for the first band wavelength makes up 80 nm). In order to reproduce the observed spectrum we need to conclude that the species dissociates in the solvent.

Table 2
TD-DFT calculations of the vertical excitation spectra from the ground state for the studied molecules.

Compound	State	λ, nm	E, eV	f	Assignment[a]
P1_monomer	T_1	454.0	2.73	–	HOMO → LUMO (95%)
	S_1	328.2	3.78	0.9790	HOMO → LUMO (96%)
	S_2	305.6	4.06	0.4349	HOMO → LUMO + 1 (91%)
	S_3	293.0	4.23	0.0939	HOMO → LUMO + 2 (90%)
	S_4	261.6	4.74	0.0381	HOMO → LUMO + 4 (77%)
					HOMO − 1 → LUMO + 2 (5%)
	S_5	257.5	4.82	0.0330	HOMO → LUMO + 3 (75%)
					HOMO → LUMO + 5 (8%)
P1_dimer	T_1	561.0	2.21	–	HOMO → LUMO (95%)
	S_1	393.4	3.15	2.1326	HOMO → LUMO (92%)
	S_2	329.5	3.76	0.0019	HOMO − 1 → LUMO (72%)
					HOMO → LUMO + 1 (17%)
	S_3	312.4	3.97	0.9795	HOMO → LUMO + 2 (61%)
					HOMO − 1 → LUMO + 1 (26%)
	S_4	311.0	3.99	0.0413	HOMO → LUMO + 1 (45%)
					HOMO − 1 → LUMO + 2 (24%)
	S_5	296.4	4.18	0.0615	HOMO → LUMO + 3 (65%)
					HOMO − 1 → LUMO + 4 (14%)
					HOMO − 1 → LUMO + 3 (10%)
P1_trimer	T_1	571.9	2.17	–	HOMO → LUMO (82%)
	S_1	410.6	3.02	3.1258	HOMO → LUMO (80%)
					HOMO − 1 → LUMO + 1 (13%)
	S_2	374.7	3.31	0.4940	HOMO → LUMO + 1 (57%)
					HOMO − 1 → LUMO (35%)
	S_3	330.2	3.76	0.2599	HOMO − 2 → LUMO (45%)
					HOMO − 1 → LUMO + 1 (33%)
	S_4	327.1	3.79	0.1358	HOMO − 1 → LUMO (37%)
					HOMO − 2 → LUMO + 1 (25%)
					HOMO → LUMO + 1 (25%)
	S_5	312.9	3.96	0.7347	HOMO − 1 → LUMO + 2 (37%)
					HOMO → LUMO + 3 (34%)
P2m	T_1	738.1	1.68	–	HOMO → LUMO (85%)
	S_1	536.5	2.31	0.4633	HOMO → LUMO (95%)
	S_2	418.2	2.96	0.5733	HOMO → LUMO + 1 (93%)
	S_3	352.1	3.52	0.1554	HOMO − 2 → LUMO (84%)
					HOMO − 3 → LUMO (6%)
	S_4	346.8	3.58	0.0592	HOMO − 1 → LUMO (97%)
	S_5	331.5	3.74	0.1957	HOMO − 3 → LUMO (88%)
P3m_monomer	T_1	482.6	2.57	–	HOMO → LUMO (89%)
	S_1	368.2	3.37	1.3322	HOMO → LUMO (90%)
	S_2	325.0	3.81	0.9070	HOMO → LUMO + 1 (95%)
	S_3	295.1	4.20	0.0269	HOMO → LUMO + 4 (90%)
	S_4	275.8	4.50	0.0605	HOMO → LUMO + 2 (93%)
					HOMO − 1 → LUMO (25%)
	S_5	268.6	4.62	0.3456	HOMO − 1 → LUMO (55%)
					HOMO → LUMO + 2 (16%)
P3m_dimer	T_1	558.4	2.22	–	HOMO → LUMO (74%)
	S_1	405.3	3.06	2.4193	HOMO → LUMO (78%)
	S_2	367.5	3.37	1.2708	HOMO → LUMO + 1 (55%)
					HOMO − 1 → LUMO (30%)
	S_3	355.2	3.49	0.7344	HOMO → LUMO + 2 (62%)
					HOMO − 1 → LUMO + 1 (23%)
	S_4	331.7	3.74	0.1279	HOMO − 1 → LUMO (43%)
					HOMO − 1 → LUMO + 1 (33%)
	S_5	299.7	4.14	0.0799	HOMO → LUMO + 3 (24%)
					HOMO → LUMO + 1 (16%)

[a] The HOMO → LUMO (96%) in the last row means that this is the main contribution to the first excitation band.

The first absorption band in the **P3m** dimer is not just a simple HOMO–LUMO transition (Table 2), but still it includes a portion of charge transfer from a backbone to the pendant substituents. This explains the lower absorption intensity of **P3m** in comparison with other related polymers of the relevant structure (Fig. 4).

A hypsochromic shift of the first absorption maximum and broaden of absorption curve of the **P2** (400 nm), **P3** (405 nm), as compared to **P1** (409 nm) is observed in UV–Vis spectra both in solution and solid state. This behavior is attributed to higher interchain interaction in **P1** in the absence of longer pendant substituents.

The PL spectra are analyzed by comparison of the structural changes in the ground singlet state and in the first excited triplet state optimized at the DFT level. The main structural changes upon electronic excitation are determined by displacements in the backbone. The C–CH=CH–C motive is changed mostly into the C=CH–CH=C structure with the corresponding deformations in the nearest phenyl rings. This is illustrated by the **P1** monomer (Figs. S2 and S3) and dimer (Figs S4 and S5) bond lengths distortion upon $S_0 \rightarrow T_1$ excitation. The largest distortions occur in the link between two monomer moieties of the dimer.

The maxima of emission in solution are shifted to longer wavelengths and centered at 450–460 nm (Fig. 4). The shift of about 50 nm can be explained by a strong deformation in the backbone. The blue shifting of polymers **P2** and **P3** with respect to **P1** observed in UV–Vis absorption spectra are also seen and exaggerated in the PL spectra (Table 1). This can be attributed to additional distortions in the triple bonds upon excitation.

We anticipate that the first excited singlet and triplet states are very close in their structure since both represent almost pure HOMO–LUMO excitation. We have predicted the phosphorescence 0–0 transition at 475 nm for **P1** monomer by the UB3LYP geometry optimization in $CHCl_3$ solvent and interpolated this value to 537 nm for polymer with account of PM3 results. (We have to remind that in Table 2 the vertical excitations calculated with the BMK functional are given.) The late method also predicts that the T_1 state of polymer is slightly more localized than the S_1 state. A small difference between the S_1 and T_1 electronic structure is represented by a slightly larger contribution (15%) of the HOMO-1 → LUMO-1 excitation to the wave function of the T_1 state in comparison with the contribution to the S_1 state (13%). See the **P1** trimer, for example (Table 2, Fig. 6c, Fig. S6).

We can conclude that LUMO is more localized than HOMO in all studied oligomers. Similar result is seen in other conjugated polymers [29]. This leads to localization of the exciton in polymers.

3.5. Electrochemical properties

The electrochemical properties of the parent and modified polymers were studied in a three-electrode electrochemical cell in deaerated acetonitrile solution containing Bu_4NClO_4 (0.1 M) as electrolyte, at room temperature. The potentials were measured against Ag/AgCl as reference electrode, using a platinum electrode disk as the working electrode. The HOMO and LUMO energy levels were estimated by cyclic voltammetry [42] in combination with the optical absorption gap (Eg) and are shown in Table 3. Ferrocene was used as internal reference and showed $E_{1/2}$ at 0.40 V vs Ag/AgCl. Using the known reference level for ferrocene, 4.8 eV below the vacuum level, the HOMO level of the polymer was determined by the equation [42]:

$$E_{\mathrm{HOMO}} = -\left(4.4 + E_{\mathrm{ox}}^{\mathrm{onset}}\right)\ (\mathrm{eV}).$$

The LUMO energy levels were estimated using the optical band gaps (E_g), $E_{\mathrm{LUMO}} = E_{\mathrm{HOMO}} + E_g^{\mathrm{op}}$ (eV).

The electrochemical oxidation onsets of **P2**, **P2m**, **P3** and **P3m** are located at 0.89V, 0.94 V, 0.93 V and 1.03 V, respectively. The HOMO level energies calculated are: −5.29 eV, −5.34 eV, −5.33 eV and −5.43 eV, respectively. The HOMO levels of all polymers are very close because polymers have the same main conjugated backbone whereas the LUMO energy levels are between −2.81 eV and −3.12 eV.

The modification of triple bond and the introduction of CN groups lowered the LUMO level of **P2** (−2.81 eV) at −3.02 eV (**P2m**) being correlated with the introduction of dicyanovinyl electron-withdrawing group in *para* position of triphenylamine

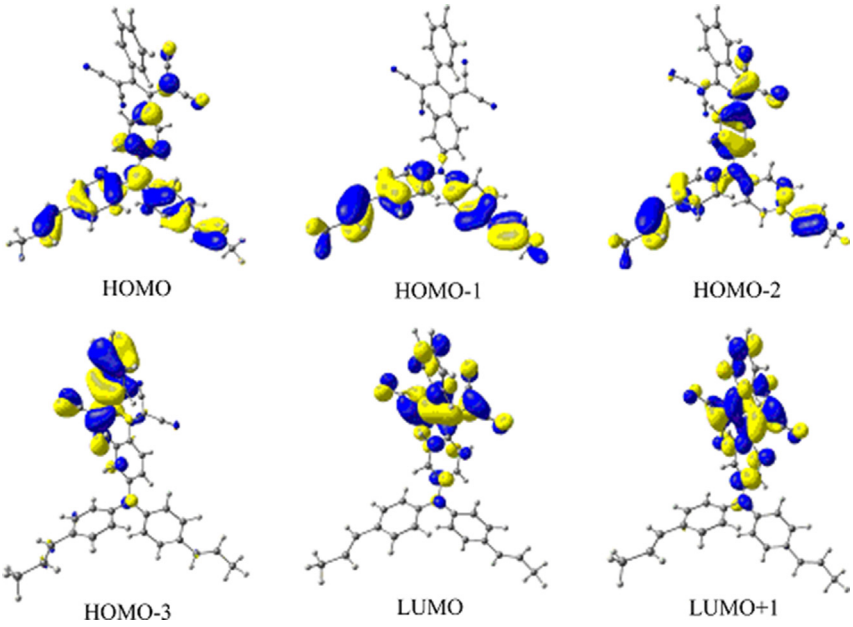

Fig. 7. DFT calculated MOs of **P2m** monomer.

moiety. For **P3** the LUMO level (−2.80 eV) has decreased at −3.12 eV (**P3m**), by chemical modification, the quaternized pyridine group being spaced by triphenylamine group by ethynylene linkage. Intramolecular charge-transfer interactions have also as effect tuning of band gap in **P2m** and **P3m**. The DFT results for the optimized geometry of the studied P1 oligomers and for the **P2m** and **P3m** monomers are presented in Table 4. HOMO for the **P2m** monomer is in a good agreement with experiment (−5.34 eV) but **P3m** is a bad model in our simulation.

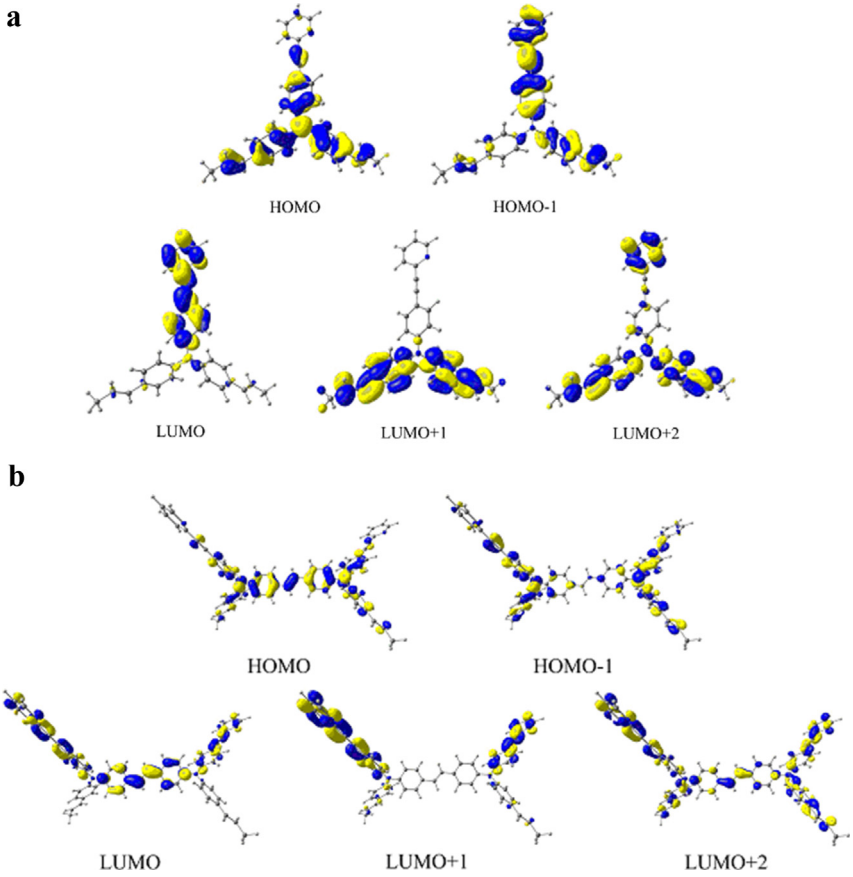

Fig. 8. (a) DFT calculated MOs of **P3m** monomer. (b) DFT calculated MOs of the **P3m** dimer.

Table 3
Electrochemical properties of polymers.

Polymer	E_g^{opt} [a] (eV)	E_{ox}^{onset} [b] (V)	E_{HOMO} [c] (eV)	E_{LUMO} [d] (eV)
P1	2.51	0.88	−5.28	−2.77
P2	2.48	0.89	−5.29	−2.81
P2m	2.32	0.94	−5.34	−3.02
P3	2.53	0.93	−5.33	−2.80
P3m	2.31	1.03	−5.43	−3.12

[a] Optical band gap estimated from the onset wavelength of optical absorption in the solid state film, $E_g^{opt} = 1240/\lambda_{onset}$.
[b] Onset potential of oxidation scan (vs. Ag/AgCl).
[c] $E_{HOMO} = -(4.8 + E_{ox}^{onset})$ (eV).
[d] $E_{LUMO} = E_{HOMO} + E_g^{opt}$ (eV).

Table 4
The DFT results for the optimized geometry of the studied **P1** oligomers and for the **P2m** and **P3m** monomers.

Compound	*E*(HOMO), eV	*E*(LUMO), eV	*E* gap
P1_monomer	−4.8276	−0.9573	3.8703
P1_dimer	−4.6469	−1.4547	3.1922
P1_trimer	−4.5852	−1.5500	3.0352
P2m	−5.3781	−3.2648	2.1133
P3m_monomer	−4.8981	−1.5813	3.3168
P3m_dimer	−4.7536	−1.7122	3.0414

HOMO for the **P2m** monomer is in a good agreement with experiment (−5.34 eV). **P3m** is a bad model in our simulation.

4. Conclusion

In summary, a series of arylenevinylene polymers containing 4,4'-triphenylamine group substituted in 4″ position with phenylethynyl- and 3-pyridylethynyl substituents, spaced by vinylene linkage, were synthesized by Stille polycondensation. The absorption and emission spectra, HOMO and LUMO energy levels and gaps energies can be fine-tuned by chemical modification of polymers using addition of tetracyanoethylene at electron-rich triple bond or by protonation and alkylation of pyridine ring. In both cases an intramolecular charge-transfer complex is formed between acceptor pendant groups and triphenylamine from conjugated chain. The variation in the absorption and emission wavelengths and redox properties of polymers after chemical modification shows the possibility of fine-tuning optoelectronic properties of arylenevinylene copolymers.

Acknowledgements

Authors (MG, AMC, TI and LV) thank to the Romanian National Authority for Scientific Research (UEFISCDI) for financial support (grant PN-II-ID-PCE-2011-3-0274, Contract 148/2011).

Appendix A. Supplementary data

Supplementary data related to this article can be found at http://dx.doi.org/10.1016/j.dyepig.2014.08.016.

References

[1] Minaev B, Baryshnikov G, Agren H. Principles of phosphorescent organic light emitting devices. Phys Chem Chem Phys 2014;16(5):1719–58.
[2] Burroughes JH, Bradley DDC, Brown AR, Marks RN, Mackay K, Friend RH, et al. Light-emitting diodes based on conjugated polymers. Nature 1990;347:539–41.
[3] Akcelrud L. Electroluminescent polymers. Prog Polym Sci 2008;28(6):875–962.
[4] Grimsdale AG, Chan KL, Martin RE, Jokisz PG, Holmes AB. Synthesis of light emitting conjugated polymers for applications in electroluminescent devices. Chem Rev 2009;109(3):897–1091.
[5] Mullen K, Scherf U. Organic light emitting devices: synthesis, properties and applications. Weinheim: Wiley-VCH; 2006.
[6] Garnier F, Horowitz G, Peng XH, Fichou D. An all-organic soft thin-film transistors with very high carrier mobility. Adv Mater 1990;2(12):592–4.
[7] Peng XZ, Horowitz G, Fichou D, Garnier F. All-organic thin-film transistors made of alpha-sexithienyl semiconducting and various polymeric insulating layers. Appl Phys Lett 1990;57(5):2013–5.
[8] Zhan X, Zhu D. Conjugated polymers for high-efficiency organic photovoltaics. Polym Chem 2010;1(4):409–19.
[9] Cheng YJ, Yang SH, Hsu CS. Synthesis of conjugated polymers for organic solar cell applications. Chem Rev 2009;109(11):5868–923.
[10] Shi W, Zhen H, Luo Y, Qin H, Mi H, Awut T, et al. Pendant-decorated polytriphenylamine derivative: potential blue-emitting and hole-transport material. Polym Bull 2010;64(1):53–65.
[11] Shi W, Wang L, Zhen H, Zhu D, Awut T, Mi H, et al. Novel luminescent polymers containing backbone triphenylamine groups and pendant quinoxaline groups. Dyes Pigments 2009;83(1):102–10.
[12] Chen YC, Hsu CY, Ho CY, Tao YT, Lin JT. Synthesis and characterization of the conjugated polymers tethered with dipolar side chains containing a benzothiadiazole entity for bulk heterojunction solar cells. Org Electron 2013;14(9):2290–8.
[13] Li Y, Zhou J, Wan X, Chen Y. Synthesis and properties of acceptor-donor-acceptor molecules based on oligothiophenes with tunable and low band gap. Tetrahedron 2009;65(27):5209–15.
[14] Stylianakis MM, Mikroyannidis JA, Dong Q, Pei J, Liu Z, Tian W. Synthesis, photophysical and photovoltaic properties of star-shaped molecules with triphenylamine as core and phenylethenylthiophene or dithienylethylene as arms. Sol Energy Mater Sol Dear Mircea Cells 2009;93(11):1952–8.
[15] Zhang ZG, Yang Y, Zhang S, Min J, Zhang J, Zhang M, et al. Effect of acceptor substituents on photophysical and photovoltaic properties of triphenylamine-carbazole alternating copolymers. Synth Met 2011;161(13–14):1383–9.
[16] Vacareanu L, Grigoras M. Synthesis and electrochemical characterization of new linear conjugated arylamine copolymers. High Perform Polym 2011;23(2):112–24.
[17] Ivan T, Vacareanu L, Grigoras M. Synthesis of poly(arylene vinylene)s containing carbazole, triphenylamine, and phenothiazine, rings in the backbone by cascade Suzuki–Heck reactions. Int J Polym Mater 2013;62(5):270–6.
[18] Kivala M, Boudon C, Gisselbrecht JP, Seiler P, Gross M, Diederich F. Charge-transfer chromophores by cycloaddition-retroelectrocyclization: multivalent systems and cascade reactions. Angew Chem Int Ed 2007;46(33):6357–60.
[19] Kato S, Kivala M, Schweizer WB, Boudon C, Gisselbrecht JP, Diederich F. Origin of intense intramolecular charge-transfer interactions in nonplanar push–pull chromophores. Chem Eur J 2009;15(35):8687–91.
[20] Shi W, Ma F, Hui Y, Mi H, Tian Y, Lei Y, et al. TCNE-decorated triphenylamine-based conjugated polymer: click synthesis and efficient turn-on fluorescent probing for Hg^{2+}. Dyes Pigments 2014;104(1):1–7.
[21] Li Y, Tsuboi K, Michinobu M. Double click synthesis and second-order nonlinearities of polystyrenes bearing donor–acceptor chromophores. Macromolecules 2010;43(12):5277–86.
[22] Tang X, Liu W, Wu J, Lee CS, You J, Wang P. Synthesis, crystal structures, and photophysical properties of triphenylamine-based multicyano derivatives. J Org Chem 2010;75(5):7273–8.
[23] Lelliege A, Blanchard P, Rousseau T, Roncali J. Triphenylamine/tetracyanobutadiene-based D-A-D π-conjugated systems as molecular donors for organic solar cells. Org Lett 2011;13(12):3098–101.
[24] Shoji T, Higashi J, Ito S, Okujima T, Yasunami M, Morita N. Synthesis of redox-active, intramolecular charge-transfer chromophores by the [2+2] cycloaddition of ethynylated 2*H*-cyclohepta [*b*] furan-2-ones with tetracyanoethylene. Chemistry Eur J 2011;17(18):5116–29.
[25] Washino Y, Michinobu T. Application of alkyne-TCNQ addition reaction to polymerization. Macromol Rapid Commununications 2011;32(8):644–8.
[26] Huang W, Chen H. Synthesis and characterization of a low-bandgap poly(-arylene ethynylene) having donor–acceptor type chromophores in the side chain. Macromolecules 2013;46(5):2032–7.
[27] Sarigiannis Y, Spiliopoulos IK. Optical and electrochemical properties of polyfluorenes with pyridine–triphenylamine bipolar unit. Polym Int 2013;62(2):196–203.
[28] Li X, Minaev B, Agren H, Tian H. Theoretical study of phosphorescence of iridium complexes with fluorine-substituted phenylpyridine ligands. Eur J Inorg Chem 2011;16:2517–24.
[29] Justino LLG, Ramos ML, Abreu PE, Charas A, Morgado J, Scherf U, et al. Structural and electronic properties of poly(9,9-dialkylfluorene)-based alternating copolymers in solution: an NMR spectroscopy and density functional theory study. J Phys Chem C 2013;117(35):17969–82.
[30] Sonntag M, Kreger K, Hanft D, Strohriegl P, Setayesh S, Leeuw D. Novel star-shaped triphenylamine-based molecular glasses and their use in OFETs. Chem Mater 2005;17(11):3031–9.
[31] Baker III TN, Doherty WP, Kelley WS, Newmeyer W, Rogers JE, Spalding RE, et al. Electrophilic substitution reactions of triphenylamine. J Org Chem 1965;30(11):3714–8.

[32] Liang Y, Feng D, Wu Y, Tsai ST, Li G, Ray C, et al. Highly efficient solar cell polymers developed via fine-tuning of structural and electronic properties. J Am Chem Soc 2009;131(22):7792–9.
[33] Hou JH, Hou LJ, He C, Yang CH, Li YF. Synthesis and absorption spectra of poly(3-(phenylenevinyl)thiophene)s with conjugated side chains. Macromolecules 2006;39(2):594–603.
[34] Kivala M, Diederich F. Acetylene-derived strong organic acceptors for planar and nonplanar push-pull chromophores. Accounts Chem Res 2009;42(2):235–48.
[35] Stefko M, Tzirakis MD, Breiten B, Ebert MO, Dumele O, Schweizer WB, et al. Donor–Acceptor (D–A)-substituted polyyne chromophores: modulation of their optoelectronic properties by varying the length of the acetylene spacer. Chem Eur J 2013;19(38):12693–704.
[36] McKusick BC, Heckert RE, Cairns TL, Coffman DD, Mower HF. Cyanocarbon chemistry. VI Tricyanovinylamines. J Am Chem Soc 1958;80(11):2806–15.
[37] Lambert C, Gaschler W, Schmalzlin E, Meerholz K, Brauchle C. Subchromophore interactions in tricyanovinyl-substituted triarylamines – a combined experimental and computational study. J Chem Soc Perkin Trans 1999;2:577–87.
[38] Becke AD. Density-functional exchange-energy approximation with correct asymptotic behavior. Phys Rev A 1988;38(6):3098–100.
[39] Lee C, Yang W, Parr RG. Development of the colle-salvetti correlation-energy formula into a functional of the electron density. Phys Rev B 1988;37(2):785–9.
[40] Frisch MJ, Trucks GW, Schlegel HB, Scuseria GE, Robb MA, Cheeseman JR, et al. Gaussian 09, Revision A.02. Wallingford CT: Gaussian Inc.; 2009.
[41] Boese AD, Martin JML. Development of density functionals for thermochemical kinetics. J Chem Phys 2004;121(8):3405–16.
[42] Bredas JL, Silbey R, Boudreaux DS, Chance RR. Chain-length dependence of electronic and electrochemical properties of conjugated systems: polyacetylene, polyphenylene, polythiophene, and polypyrrole. J Am Chem Soc 1983;105(22):6555–9.